

# Root Growth of Carbon and Boron Nitride Nanotubes in Plasma of High Pressure Arc

I. D. Kaganovich, A. Khrabry, B. Greenberg, S. Ethier, A. Pineda, S. Yatom, Y. Raitses

Princeton Plasma Physics Laboratory, Princeton NJ 08542

**Abstract:** In our previous experiments we synthesized boron nitride (BNNTs) and carbon nanotubes (CNTs) in volume by anodic arc discharges at near atmospheric pressure of nitrogen and helium, respectively. In order to understand NTs formation, we determined the plasma and gas composition in the nucleation and growth regions using laser diagnostics, atomistic simulations, thermodynamic and fluid dynamics (CFD) modeling. This integrated and validated modeling strongly suggests root growth mechanisms for both BNNTs and CNTs.

**Keywords:** boron nitride nanotubes, carbon nanotubes, anodic arc.

## 1. Synthesis of carbon nanotubes in anodic arc

This work reports on studies of arc-based synthesis of carbon and boron nitride nanomaterials. Applying a set of the in-situ diagnostics of plasma and nanoparticles, our synthesis experiments revealed that the carbon arc forms a highly inhomogeneous plasma consisting of distinguishable regions with different dominant species, including ions, atoms, molecules and clusters, and nanoparticles. Measurements revealed clouds of nanoparticles in the arc periphery bordering the region with a high density of diatomic carbon molecules, as shown in Fig.1 from Ref.[1] based on planar laser induced incandescence (LII) technique. Two-dimensional computational fluid dynamics (CFD) simulations of the arc combined with thermodynamic modeling show that this is due to the interplay of the condensation of carbon molecular species and growth of nanoparticles carried by the convection flow pattern.

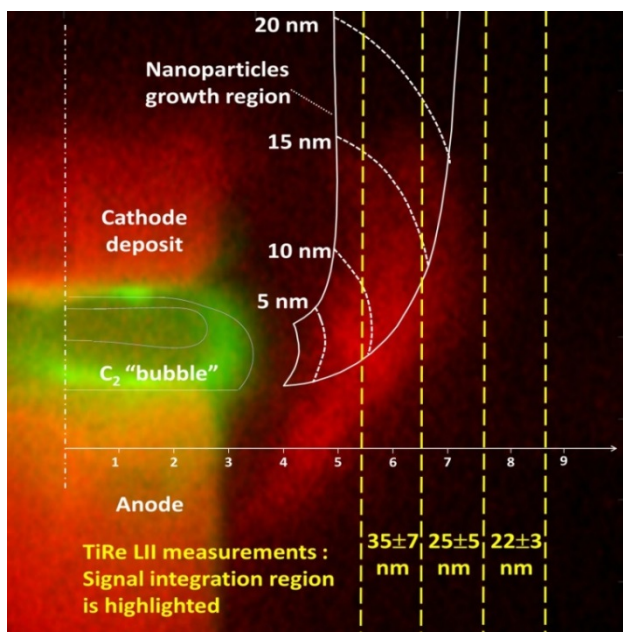


Fig. 1. Comparison of measured and simulated carbon nanoparticles location and sizes in the arc periphery. Results of the simulations are shown by white lines overlaid on the experimental photo. Locations where

nanoparticles have specific average sizes are shown by white dashed lines. Yellow dashed lines indicate the locations of the signal line integration in measurements of the nanoparticle average diameter using time-resolved LII method. Areas from which a LII signal was collected are highlighted and the mean particle diameter for each area is shown. Image courtesy of Ref.[1]. Simulations results for the nanoparticles sizes and location region are in a good agreement with the measurements.

Corresponding gas composition and plasma density are shown in Fig.2.

## Chemical composition and growth of nanoparticles

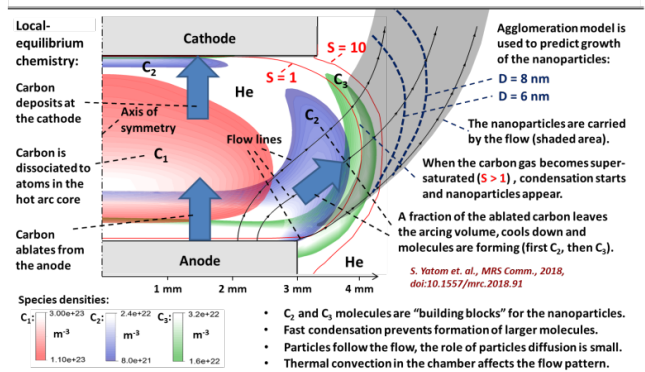
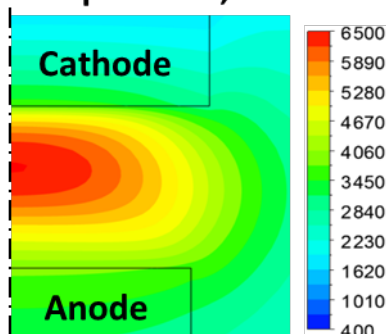
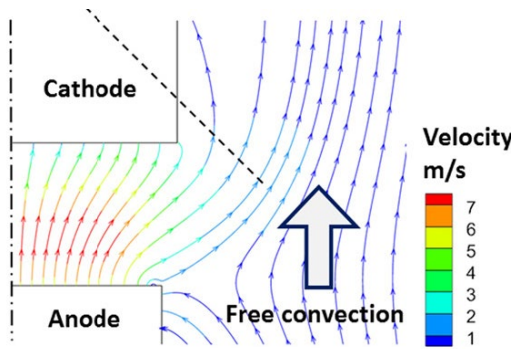


Fig.2 Schematics of carbon species evolution in arc from Ref.1.

## Temperature, K





**Flow pattern (velocity streamlines)**

Fig.3 Simulation of gas temperature, flow pattern and gas velocity in the arc from Ref.1.

From CFD simulations it follows that the temperature along the nanoparticle growth region changes from 3500 K at the beginning where nanoparticle nucleate to about 2000 K on the distance of length  $L \approx 1$  cm - the characteristic length of the nanoparticle growth region, width of this region is  $W \approx 3$  mm. Therefore, typical time for nanoparticle growth is about  $L/v$  where gas flow velocity is about 1m/s giving. Note that this is many orders of magnitude longer as compared to time scale of atomistic processes.

To investigate in more details the process of carbon condensation, we performed Density Functional Theory Tight-Binding (DFTB+) simulations<sup>2</sup> of carbon condensation<sup>3</sup>. The simulation box was a cube with width 100Å where 1000 atoms were placed. This corresponded to artificially increased pressure of  $\sim 1000$ atm needed to speed up the calculation and make sure carbon atoms had time to collide and interact with each other. A snapshot of a typical evolution is shown in Fig. 4.

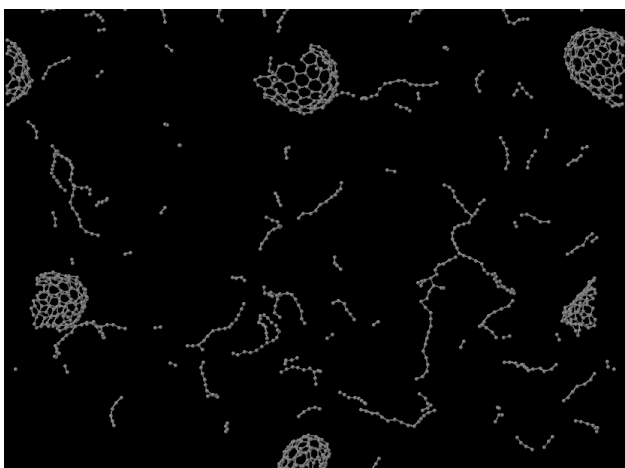


Fig.4. DFTb simulations of carbon vapor condensation at gas temperature  $T=3000$ K. Initial set up of simulations is courtesy of Longtao Han.

Carbon atoms quickly assemble into long chains. At certain length, chains convert into carbon flakes and then they form fully developed fullerenes. Note that given enough time in atomistic simulations all remaining chains will collide and fully assemble into fullerenes, see more details in Ref.3.

To confirm this we also used a thermodynamic code to explore evolution of the carbon chain length as a function of temperature. The code uses the Gibbs energy minimization principle to find the equilibrium state of the system at given temperature and pressure. The Gibbs free energies of formation for chains of length 1-5 are given in NIST database<sup>4</sup>; and we approximated the Gibbs energy for longer chains using a simple model, as shown in Fig.5.

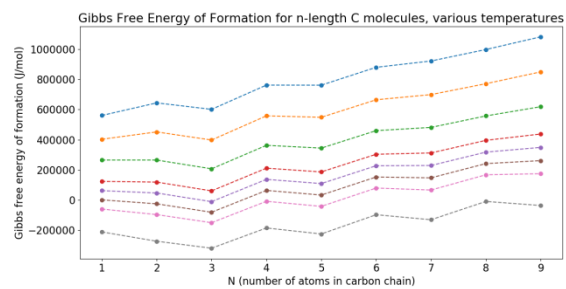
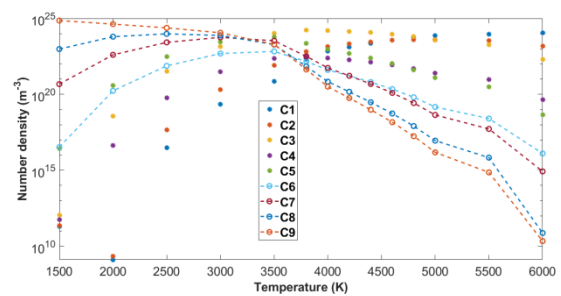


Fig.5 The Gibbs energies of formation for carbon chains used in the thermodynamic modeling.

Based on this approximation, we made a prediction for the composition of carbon gas species at atmospheric pressure as a function of temperature, which is shown in Fig.6.

(a)



(b)

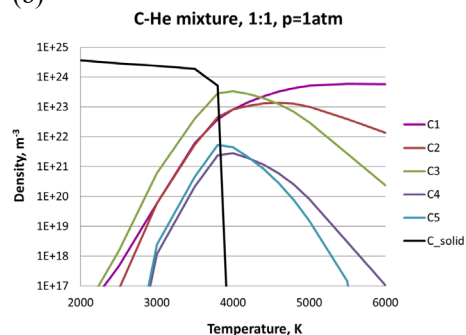


Fig.6. Predicted equilibrium composition at 1 atm. carbon pressure (a) if only 9 first molecules are taken into account. (C1-9 linear chains, If we account for longer

chains, the longest chain will dominate the composition at  $T < 3000\text{K}$ .), (b) if only 5 first molecules are taken into account. (C1-5 linear chains) and solid carbon.

As evident from Fig.6, at a temperature of 3000K, where CNT are thermally stable<sup>5</sup>, carbon condenses into the longest chains available for simulations and then rolls into flakes and further converts into fullerenes. Therefore, in the real system carbon will condense into stable large carbon particles, as seen in Fig.4 from DFTB simulations at temperature below 3000K, which is much higher than temperature where CNTs form. These findings are consistent with previous studies of Refs. [6,7].

*This also means that previous studies (see, e.g., Ref. [8] and references within) that assume that carbon atoms are readily available for CNT formation in the arc at temperatures about 2000K are called into question. Therefore, the only carbon available for CNT formation is the carbon dissolved into metal catalyst particles and the synthesis scheme should be devised in such a way that metal catalyst particles are continuously available in the temperature range 2000-3000K, for example, combination of high melting point catalyst particles: cobalt and nickel. This also strongly support root growth mechanism model.*

## 2. Synthesis of boron nitride nanotubes in anodic arc

For production of BNNTs, a boron is evaporated in the near-atmospheric-pressure arc in nitrogen atmosphere<sup>9</sup>. BNNTs were synthesized by a dc arc discharge in a pure nitrogen environment at 400 Torr. The cathode and the anode of the arcs were made from lanthanated tungsten rods of 3.125 mm diameter and 6.35 mm diameter, respectively. The arc was generated by briefly bringing the cathode and the anode in contact, after which the current was maintained at 40 A. An external control system increased the electrode gap until the specified discharge voltage (35–40 V) was reached. This voltage includes the voltage drop across the arc and along the electrodes. The gap between the electrodes did not exceed 1 cm wide. A 99.9% boron target with 0.1% of metal impurities was immersed into the hot plasma region of the arc discharge. No metallic catalyst was added. The target evaporated providing boron feedstock for synthesis of BN nanoparticles, including BNNTs. Transmission electron microscopy (TEM) samples were prepared by sonicating the acetone solution that contains the white synthesized products for 2 minutes. The morphology of the synthesized products was studied by using an FEI Talos scanning transmission electron microscope operated at 200 kV. The chemical analysis on the synthesized materials was performed using energy dispersive X-ray spectroscopy (EDS).<sup>9</sup>

To determine the gas composition at regions where BNNTs are formed, in our previous paper<sup>10</sup>, we

performed thermodynamic calculations for chemical composition of mixture of boron and nitrogen at atmospheric pressures with and without addition of hydrogen. A broad set of B, N and H containing gas species from [11] was considered with thermodynamic data from Refs. [12] and [13]. Liquid boron and solid BN were taken into consideration as well. This allowed us to account for condensation of boron and determining the conditions for solid BN formation, see Fig. 7.

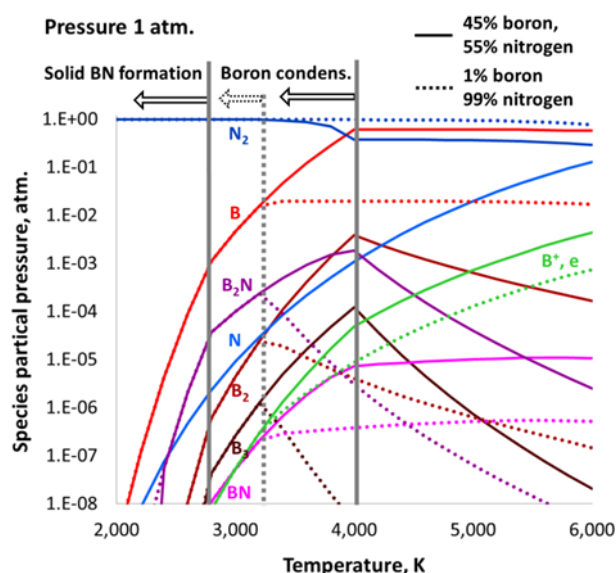


Figure 7. Composition of B-N mixtures at 1 atm.. Shown are partial pressures of gas phase species as functions of temperature for boron to nitrogen ratios 45 to 55 (solid lines) and 1 to 99 (dotted lines).

In this calculations boron condensation is taken into account; temperatures of boron condensation and solid BN formation are shown with vertical grey lines. Fraction of boron within the mixture affects composition of the gas species only at higher temperatures, before boron condensation starts. When the condensation takes place, gas species composition is determined merely by the boron vapor saturation curve. At the temperature of solid BN formation,  $B_2N$  has the highest density among nitrogen containing species, after  $N_2$ , and can be suggested as major source of nitrogen for formation and growth of BNNTs. According to our DFT simulations BNNT is stable on liquid boron droplet at temperature of 2000K. However, BN containing radical density is too low at temperature of 2000K to allow for direct synthesis of BNNTs from BN radicals or its derivatives (where BNNT should form as it was predicted by DFT simulations of our previous study<sup>9</sup>). Similarly to the CNT case, the more probable scenario to explain observed yield of BNNTs is to assume accumulation of BN radicals on the surface of liquid boron droplets while the gas cools from 4000K to about 2000K and where droplets form, see Fig.8.

*This also means that previous studies (see, e.g., Ref. [14] and references within) that assume that BN radicals are*

readily available for BNNT formation in the arc at temperatures around 2000K are called into question.

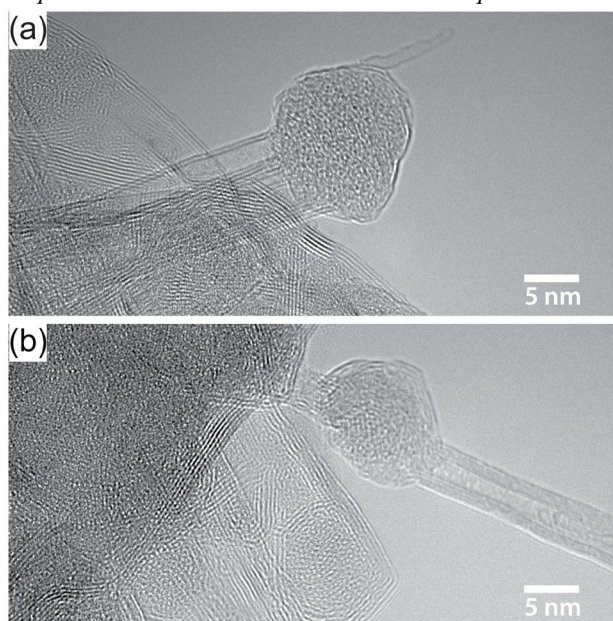


Fig.8. Post-synthesis high-resolution TEM images showing BNNTs attached to a boron nanoparticle. The BN material is obtained from an arc discharge synthesis. From Ref.[9].

The arc modeling was supported by the US DOE Office of Science, Fusion Energy Sciences. Experiments and simulations of synthesis processes were supported by the US Department of Energy (DOE), Office of Science, Basic Energy Sciences, Materials Sciences and Engineering Division.

<sup>1</sup> S. Yatom, A. Khrabry, J. Mitrani, A. Khodak, I. Kaganovich, V. Vekselman, B. Stratton and Y. Raiteses, "Synthesis of nanoparticles in carbon arc: measurements and modeling", MRS. Communications **8**, 842-849 (2018).

<sup>2</sup> <https://www.dftb.org/about-dftb/>

<sup>3</sup> B. Greenberg, I. D. Kaganovich, A. Khrabry, S. Ethier, "Simulations of Carbon Vapor Condensation", to be submitted to Carbon (2019).

<sup>4</sup> Malcolm W. Chase, Jr. NIST-JANAF Thermochemical Tables. American Chemical Society; American Institute of Physics for the National Institute of Standards and Technology, 1998.

<sup>5</sup> K. M. Liew, C. H. Wong, X. Q. He, and M. J. Tan, "Thermal stability of single and multi-walled carbon nanotubes", Phys. Rev. B **71**, 075424 (2005).

<sup>6</sup> G. Cota-Sanchez, G. Soucy, A. Huczko, H. Lange, "Induction plasma synthesis of fullerenes and nanotubes using carbon black-nickel particles" Carbon **43**, 3153-3166 (2005).

<sup>7</sup> WeiZong Wang, MingZhe Rong, Anthony B Murphy, Yi Wu, Joseph W Spencer, Joseph D Yan and Michael T C Fang, "Thermophysical properties of carbon-argon and

carbon-helium plasmas", J. Phys. D: Appl. Phys. **44** 355207 (2011).

<sup>8</sup> Oleg A. Louchev and Hisao Kanda, Arne Rose'n and Kim Bolton, "Thermal physics in carbon nanotube growth kinetics", Journal of Chemical Physics **121**, 446 (2004).

<sup>9</sup> B. Santra, H.-Y. Ko, Y.-W. Yeh, F. Martelli, I. Kaganovich, Y. Raiteses, R. Car. "Root-growth of boron nitride nanotubes: experiments and *ab initio* simulations". Nanoscale (2018) DOI: 10.1039/C8NR06217J (2018).

<sup>10</sup> Alexander Khrabry, Igor D. Kaganovich, Shurik Yatom, Vlad Vekselman, Jelena Radić-Perić, John Rodman, Yevgeny Raiteses, "Determining Gas Composition for Growth of BNNTs Using Thermodynamic Approach", arXiv:1810.09586.

<sup>11</sup> J. Radic-Peric, "Thermodynamic modelling of boron nitride formation in thermal plasma". Mater. Sci. Forum **518** (2006) 349-354.

<sup>12</sup> "NIST-ANAF Thermochemical tables", Journal of Physical and Chemical Reference Data, Fourth Edition, Malcolm W. Chase, Jr., 1998.

<sup>13</sup> J.M.L. Martin, J.P. François, R. Gijbels. "Ab initio study of boron, nitrogen, and boron-nitrogen clusters. I. Isomers and thermochemistry of B<sub>3</sub>, B<sub>2</sub>N, BN<sub>2</sub>, and N<sub>3</sub>", The Journal of Chemical Physics **90** (1989) 6469-6485.

<sup>14</sup> P.S. Krstic, L. Han, S. Irle, H. Nakai, "Simulations of the synthesis of boron-nitride nanostructures in a hot, high pressure gas volume", Chem. Sci. **9**, 3803-3819 (2018).